Proceedings of the 21st ICSMGE, Vienna, Austria, 14 – 19 June 2026. Pistrol, Adam & Schweiger (eds.)
Published by: ÖGG, Austrian Society for Geomechanics, Salzburg, Austria, ISBN 978-3-9503898-4-5
https://doi.org/10.53243/ICSMGE2026-910

Fabric-Aware Foundation Design in Metastable Glaciogenic Silts: A Dual-Site Case History

Ri Hong Kee, Andy O'Sullivan
Andy O'Sullivan Geotechnical Engineering, Auckland, New Zealand, cyrus@aosullivan.co.nz

Sergei Terzaghi
Andy O'Sullivan Geotechnical Engineering (Australia), Katoomba, NSW, Australia

ABSTRACT: Foundation design in fine-grained soils often relies on conventional strength indices such as undrained shear strength (s_u) and Standard Penetration Test (SPT) blow counts. However, in metastable glaciogenic silts, these parameters can mask a high sensitivity to destructuration. This paper presents an anonymized case history of two bridge sites located on similar fines-rich, low-plasticity silt deposits with high in-situ void ratios ($e_0 \approx 0.88 – 0.96$). At the first site, high-energy impact driving with plugged piles caused extensive remolding of the soil fabric, leading to significant settlement (> 160 mm) despite the piles meeting nominal capacity requirements. Conversely, at the second site, vibratory open-ended installation preserved the soil microstructure, resulting in negligible settlement and superior set-up rates. Through the integration of dual-rate cone penetration testing (CPT), seismic dilatometer (sDMT) profiling, and high-strain dynamic testing, this study demonstrates that performance in these deposits is governed by state parameter (ψ) and fabric preservation rather than initial strength. A "fabric-aware" design workflow is proposed, emphasizing the use of installation method as a primary design variable to ensure reliable long-term performance in sensitive intermediate soils.

KEYWORDS: Glaciogenic silt; Pile installation effects; Critical state soil mechanics; In-situ testing

1 INTRODUCTION

Conventional pile design generally follows well-established total and effective stress frameworks, commonly known as the alpha and beta methods. In these approaches, shaft and toe resistances are calculated using empirical correlations to undrained shear strength (s_u) or effective overburden stress, with input parameters frequently derived from Standard Penetration Test (SPT) blow counts or basic strength index properties (API, 2014; Brown et al., 2010). While these methods provide a robust baseline for typical clays and sands, they often oversimplify behavior in complex intermediate soils.

In many natural silts and soft clays, performance is governed less by composition than by microstructure and in-situ state. Where soils are metastable, lightly bonded, anisotropic, and deposited at relatively high void ratios, small-strain stiffness can be deceptively high, while undrained and cyclic behavior remains strongly contractive once the fabric is disturbed (Høeg et al., 2000; Yamamuro & Lade, 1998). Consequently, standard parameter sets that ignore fabric and rate effects can give a misleading impression of reliability (Thevanayagam et al., 2002; Jefferies & Been, 2016).

Glaciogenic silts provide a clear example of this duality. Rock flour generated by glacial grinding and redeposited as fines-rich, low-plasticity silt tends to form an open packing with angular grains and weak physico-chemical bonding. At working stresses, these materials often exist above their critical-state line with a positive state parameter (ψ), yet exhibit high shear-wave velocity (Vs) and small-strain shear modulus (G0) due to the stiffness of the intact fabric. However, once bonds are broken by pile installation or cyclic loading, the soil behaves as a contractive, sand-like silt with limited undrained strength (Thevanayagam, 2000).

This paper addresses the gap between conventional practice and the behavior of fabric-sensitive silts using an anonymized bridge foundation case history. Two contrasting installation strategies were employed on similar stratigraphy: Site A utilized impact-driven, plugged piles, while Site B utilized vibratory, predominantly open-ended installation. The resulting dataset allows for a direct comparison between "fabric-blind" and "fabric-aware" design outcomes.

2 SOIL SETTING AND MATERIAL CHARACTERISATION

2.1 *Regional Setting and Stratigraphy*

The case history concerns a bridge foundation system located on a low-relief coastal plain underlain by complex glaciofluvial and glaciolacustrine deposits. In this environment, glacially derived rock flour has been reworked by fluvial processes and standing water, forming interbedded sequences of gravel, sand, and fines-rich silt.

Subsurface investigations at the project sites reveal a consistent stratigraphic sequence. The profile is characterized by a near-surface crust of loose to medium-dense sandy gravel, underlain by medium-dense to very dense sandy gravel, which caps a laterally continuous fine-grained unit of firm to very stiff silt extending to significant depth.

A representative geological profile is summarized in Figure 1, delineating the transition from the upper granular crust to the underlying sensitive silt unit.

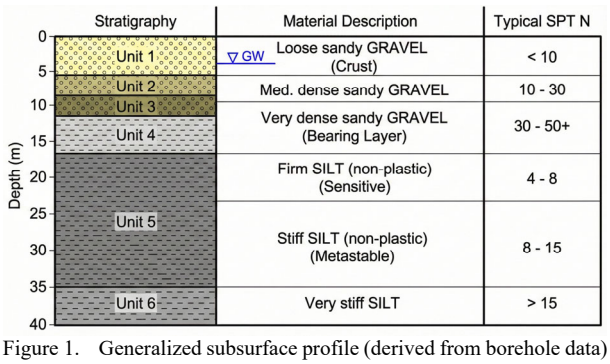

Figure 1. Generalized subsurface profile (derived from borehole data)

Standard Penetration Test (SPT) N-values effectively highlight the sharp contrast in consistency. The upper gravels show a rapid increase in resistance, with N-values rising from less than 10 in the shallow loose material to exceeding 30 (often reaching refusal, 50+) in the densified gravel layers. The underlying silts return N-values that would conventionally be

interpreted as "firm" to "very stiff" (typically 4 to 15, locally higher). While such values might imply competence within traditional total-stress design frameworks, they mask the sensitivity of the deposit confirmed by advanced testing. Groundwater was recorded between 2.7 m and 4.6 m below ground level, indicating that the silt unit is fully saturated within the zone of pile influence.

2.2 *Index Properties and Microstructure*

Laboratory classification confirms that the deeper fine-grained formation is a fines-rich, low-plasticity silt (ML). Particle size distribution (PSD) analyses indicate a fines fraction (particles passing 63 μm) generally between 80% and 95%, with a minor sand fraction and negligible gravel content.

The particle size characteristics are summarized in Figure 2, which illustrates the predominantly silty nature of the deposit.

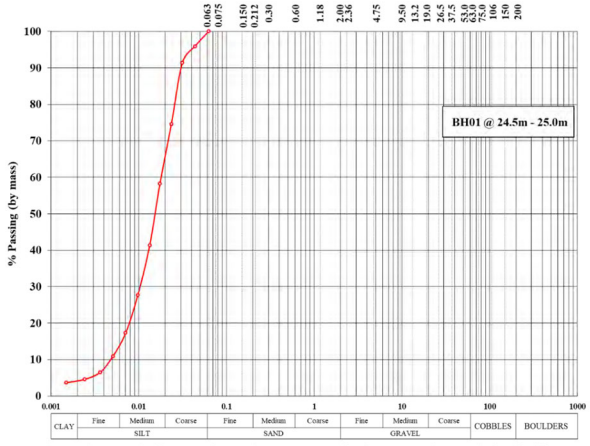

Figure 2. Particle Size Distribution (PSD) summary indicating high fines content.

Natural water contents for the critical silt unit typically range from 33% to 36%10. Corresponding in-situ void ratios (e_0) generally fall between 0.88 and 0.96, indicating a very loose structure relative to the material's critical state.

Plasticity testing revealed non-plastic to slightly plastic behavior; many samples exhibited dilatancy during handling, and where Atterberg limits could be determined, the Plasticity Index (PI) was consistently less than 7. The clay mineral content is minimal (<14), confirming that the material behaves mechanically as a granular silt rather than a cohesive clay.

Microstructurally, these glaciogenic silts comprise angular grains with open packing, supported by weak physico-chemical bonding and flocculated contacts. This fabric generates an elevated small-strain stiffness in the intact state but is metastable; once these weak bonds are broken by high-strain shearing (such as pile driving), the structure collapses, leading to significant strength loss.

2.3 *Critical State Indicators and Contractive Tendency*

Critical State Soil Mechanics (CSSM) provides the necessary framework for interpreting the behavior of these low-plasticity deposits. Research on similar silts suggests that the critical state void ratio (e_{cs}) at typical working stresses lies around 0.70 (Jefferies & Been, 2016).

Comparing the field data to this benchmark reveals a precarious in-situ state. With in-situ void ratios of 0.88 to 0.96 sitting well above the critical state value of 0.70, the soil exists in a very loose state with a strongly positive state parameter ($\psi > 0$)

Cyclic triaxial testing on reconstituted samples confirms this vulnerability. Under cyclic stress ratios (CSR) representative of transient train loading (≈0.025), samples exhibited rapid pore pressure accumulation and contractive behavior. As shown in Figure 3, the sample exhibited positive excess pore pressure generation under repeated loading cycles.

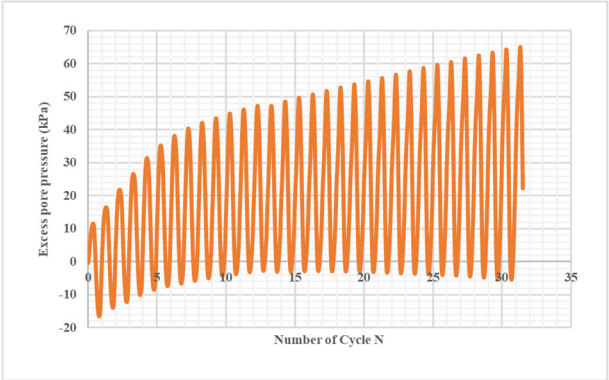

Figure 3. Cyclic triaxial test results showing excess pore pressure generation under cyclic loading (CSR = 0.025), confirming contractive tendency.

While monotonic tests on disturbed specimens showed a transition to dilative behavior at large strains (consistent with densification towards the CSL), the intact fabric remains prone to cyclic liquefaction or "cyclic mobility" phenomena.

2.4 *Shear Wave Velocity and Small-Strain Stiffness*

The disparity between the "firm" SPT classification and the loose void ratio is best reconciled through small-strain stiffness measurements. Seismic dilatometer (sDMT) and MASW surveys recorded shear wave velocities (Vs) in the silt typically ranging from 200 m/s to 350 m/s.

Using the fundamental relationship $G_0 = \rho Vs^2$, the derived small-strain shear modulus is significantly higher than would be predicted by void ratio and effective stress alone. This "stiffness bonus" is attributed to the metastable fabric and weak cementation discussed in Section 2.2.

Crucially, this stiffness is fragile. Post-construction sDMT profiling demonstrated a distinct reduction in Vs of 20–30% in the zones adjacent to driven piles compared to pre-installation baselines. This degradation is clearly visualized in Figure 4, which compares pre-installation (sDMT-C) and post-installation (sDMT-D) velocity profiles.

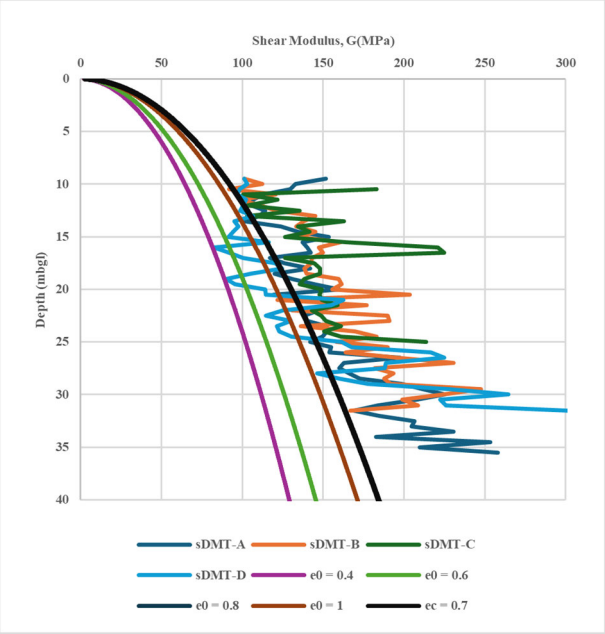

Figure 4. Shear wave velocity (Vs) profiles from sDMT, illustrating the degradation of soil fabric (reduction in stiffness) post-installation.

This degradation of G_0 provides field-scale evidence of destructuration: the impact driving process shattered the inter-particle bonds, collapsing the open fabric and reducing the soil to a remolded, contractive state.

2.5 *Summary of Key State Indicators*

On the basis of the project data, the silt formation can be characterized as follows:

- Classification: Fines-rich (>80%), low-plasticity (PI <7) granular silt, governed by state rather than cohesion.
- State: High void ratios ($e_0 \approx 0.88 – 0.96$) relative to the critical state ($e_{cs} \approx 0.70$), implying a positive state parameter (ψ) and strong contractive tendency.
- Stiffness: High initial Vs (200 – 350 m/s) driven by metastable bonding, which is lost upon high-strain disturbance.
- Sensitivity: A distinct "sand-like" behavior where performance is dictated by the preservation or destruction of the soil fabric.

These characteristics explain why conventional investigations indicated competent ground, yet pile installation triggered significant destructuration. The following section details how these microstructural features manifested during dual-rate in-situ testing and pile installation.

3 IN-SITU TESTING AND RATE-DEPENDENT RESPONSE

3.1 *Investigation and Testing Programme*

To characterize the metastable silt described in Section 2, the field investigation moved beyond standard index testing to explicitly target rate effects and fabric sensitivity. The programme integrated three advanced testing modes:

1. Paired Dual-Rate Piezocone Testing (CPT-A vs. CPT-B): Co-located soundings were performed to decouple drainage effects from stratigraphy. Standard penetration (20 mm/s) was compared against slow penetration (≈ 0.3 mm/s) to bound the undrained and partially drained responses.
2. Seismic Dilatometer Testing (sDMT): Vs profiling was utilized to define the small-strain stiffness baseline (G_0) and, crucially, to map changes in soil fabric before and after pile installation.
3. High-Strain Dynamic Pile Testing (PDA): Carried out on production and test piles to derive segmental shaft resistance distributions and quantify set-up behavior over time.

3.2 *Dual-Rate CPT Response: The "False Weakness" Paradox*

The paired CPT data reveal a distinct rate-dependence within the glaciogenic silt that is not apparent from SPT N-values alone. Figure 5 presents a representative comparison, overlaying standard-rate and slow-rate traces.

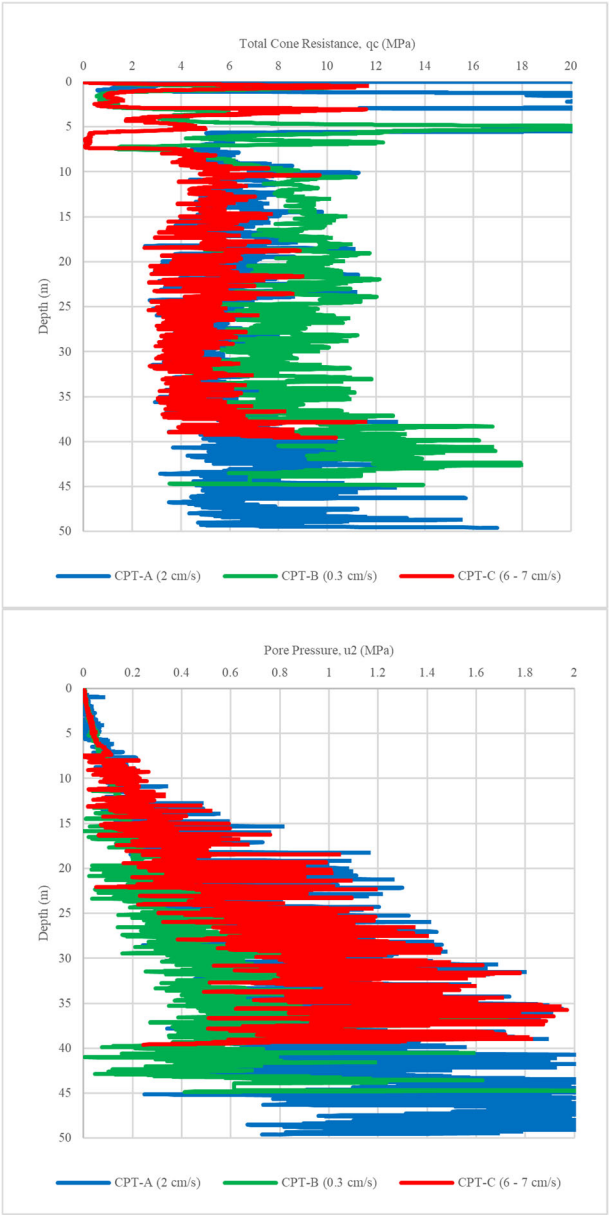

Figure 5. Comparison of standard rate (20 mm/s) vs. slow rate (3 mm/s) CPT responses. Note the suppressed resistance (q_c) and elevated

pore pressure (u_2) in the standard test, indicative of undrained remolded behavior.

Three consistent trends emerge from the dataset:

1. Suppressed Resistance at Standard Rates: The standard CPT-A consistently records lower tip resistance compared to the slow-rate CPT-B ($q_{t,slow} \approx 1.5\ x\ q_{t,std}$).
2. Elevated Pore Pressures: The standard rate generates high excess pore pressure (Δu), driving the pore pressure ratio (B_q) up. Conversely, the CPT-B records significantly lower u_2, indicating partial drainage and reduced fabric damage.
3. State Interpretation: When plotted in effective stress space, the standard CPT-A data reflects a remolded, undrained residual state, while the CPT-B approximates the intact, drained strength.

Implication: Relying solely on standard CPT-A correlations would misclassify this high-void-ratio silt as a weak cohesive material, masking its potential for high static stiffness while simultaneously failing to identify its extreme sensitivity to dynamic destructuration.

3.3 *sDMT as a "Damage Meter" for Installation Effects*

While CPT rates highlight intrinsic soil sensitivity, sDMT profiling provided a direct measure of induced damage at the impact-driven site (Site A). Shear wave velocity (Vs) profiles obtained pre- and post-installation quantified the extent of destructuration caused by the driving energy.

Impact Driving with Plugged Toes (Site A): As shown in Figure 6, a distinct "damage zone" was detected adjacent to the driven piles. Vs values within the silt unit dropped by approximately 20 – 30% relative to the pre-installation baseline.

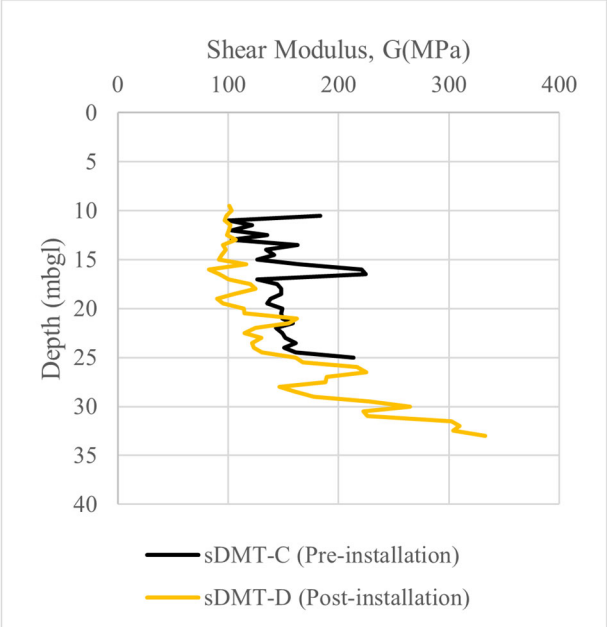

Figure 6. Pre- and Post-installation shear wave velocity profiles adjacent to impact-driven piles at Site A. The reduction in Vs (orange line) relative to the baseline (black line) quantifies the destructuration of the silt fabric.

This 20 – 30% reduction in Vs corresponds to a ≈ 40 – 50% loss in small-strain shear modulus (G_0). This confirms that high-energy impact driving with a closed toe acts as a remolding agent, shattering the delicate physio-chemical bonds described in Section 2 and reverting the soil to a contractive residual state.

3.4 *Dynamic Pile Testing: The "Test Pile" Experiment*

The link between fabric preservation and pile capacity was established through comparative Dynamic Pile Testing (PDA).

The Open-Ended vs. Closed-Ended Contrast (Site A): The most compelling evidence comes from a unique "Test Pile" experiment involving the conversion of an open-ended pile to a closed-ended (plugged) pile. Initial PDA testing on the open-ended pile (6 days setup) showed robust skin friction, particularly in the lower silt unit (approx. 70 kPa). However, once the pile was converted to a closed-ended configuration (simulating a plug) and re-driven, the skin friction at the base collapsed to near zero (Figure 7).

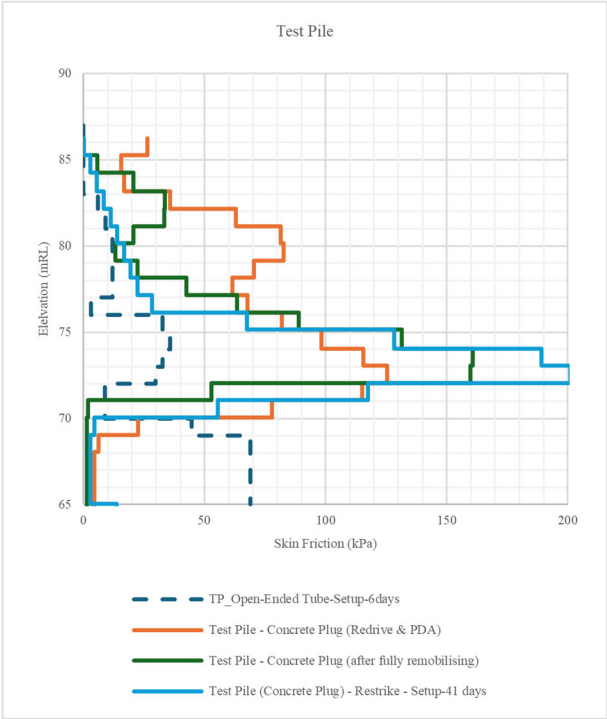

Figure 7. Degradation of unit shaft resistance derived from PDA signal matching. Note the dramatic loss of capacity in the lower silt unit after the pile was converted from open-ended (dashed line) to plugged (solid lines), inducing large-strain remolding.

Set-up Rates an Installation Method (Site A vs. Site B): Comparing the two sites reveals the long-term consequences of this destructuration. As shown in Figure 8, piles installed via vibratory methods (Site B) exhibited a set-up rate approximately four times faster than the driven piles at Site A (1.1 kPa/day vs. 0.27 kPa/day).

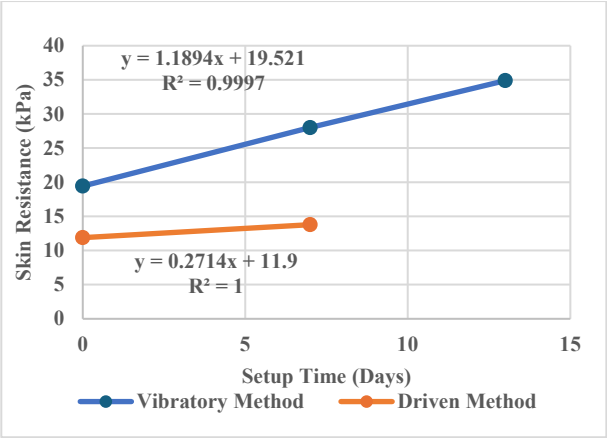

Figure 8. Comparison of skin resistance development over time. Vibratory installation (blue dots) demonstrates superior capacity and faster set-up compared to impact driving (orange dots).

This data strongly suggests that the vibratory method preserved the soil fabric (consistent with the intact CPT-B response), whereas the impact driving created a remolded zone with significantly retarded strength gain.

3.5 *Synthesis of Field Observations*

The combined evidence supports a single, coherent behavioral model for these glaciogenic silts:

1. Intact State: The soil possess a stiff, metastable fabric (High Vs, High CPT-B qc).
2. Destructured State: High-strain shearing – whether by a plugged pile or standard CPT – collapses this fabric, generating excess pore pressure and reducing the soil to a contractive, weak residue.
3. Design Consequence: The choice of installation method dictates the final state of the soil. Impact driving (Site A) degrades the soil to its residual state, while vibratory installation (Site B) maintains the "stiffness bonus" of the intact fabric.

4 DESIGN INTERPRETATION AND LESSONS LEARNED

4.1 *Fabric-Blind vs. Fabric-Aware Performance*

The divergence in performance between two sites illustrates the critical role of installation method in sensitive silts. If interpreted through a conventional, "fabric-blind" $\alpha - \beta$ framework, both sites appeared competent, with SPT N-values and initial static calculations suggesting adequate capacity. However, the operational reality revealed a fundamental difference in soil state post-installation.

Site A (Fabric-Blind Outcome): The impact-driven, plugged piles caused extensive remodeling of the pressure bulb beneath the toe. Significantly, the piles failed to achieve the required geotechnical capacity at the original design depths. The design was forced to react by extending the piles deeper to mobilize sufficient nominal resistance.

Despite eventually meeting the static capacity requirements through these extensions, the foundation experienced significant settlement under service loads. Monitoring data reveals a rapid accumulation of vertical displacement, stabilizing at approximately 160mm.

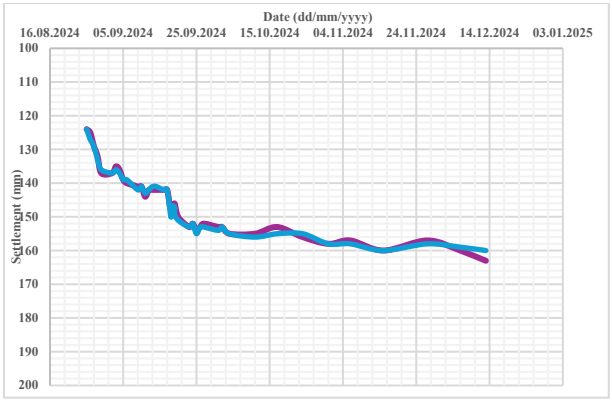

Figure 9. Measured pile-cap settlement at Site A (Impact Driven), showing stabilization at approximately 160 mm.

This outcome highlights a critical failure in the conventional approach: satisfying Ultimate Limit State (ULS) capacity via extension did not ensure Serviceability Limit State (SLS) performance. The settlement correlates strongly with a volumetric collapse mechanism within the remolded zone. Using the void ratios established in Section 2 ($e_0 \approx 0.9$) and a critical state void ratio ($e_{cr} \approx 0.7$), the theoretical settlement (S) for a remolded zone of thickness H (1.0D to 1.5D) beneath the toe is calculated as:

$$S = \frac{H(e_0 - e_{cr})}{1 + e_0}$$

Substituting the site-specific parameters yields a predicted settlement range of 126mm to 189 mm. The observed 160 mm falls precisely within this bound, confirming that the failure mechanism was the collapse of the metastable fabric triggered by the installation method, a phenomenon that deeper driving likely exacerbated rather than mitigated.

Site B (Fabric-Aware Outcome): In contrast, the vibratory, open-ended piles at Site B preserved the soil structure. Survey monitoring (Figure 10) indicates negligible vertical displacement, fluctuating within a few millimeters of the initial levels.

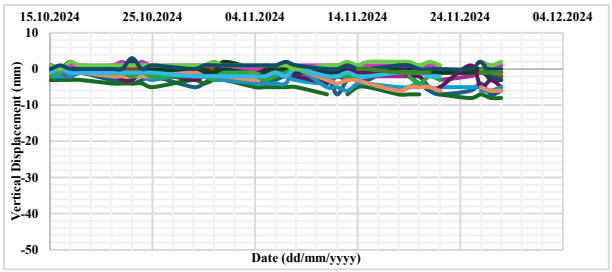

Figure 10. Survey monitoring results at Site B (Vibratory), showing stable performance with negligible vertical displacement.

This stability is consistent with the "preserved fabric" model: because the soil was not remolded into a contractive state, the foundation behaves as a stiff, shaft-dominated system supported by the intact small-strain stiffness (G_0) identified in the sDMT surveys.

4.2 *Recommended Workflow for Sensitive Glaciogenic Silts*

Drawing on these observations, a "fabric-aware" design workflow is proposed for similar metastable deposits:

1. Recognize Metastability: Use index properties (High e_0, Low PI, High Fines) to flag potential sensitivity. If $e_0 > e_{cr}$, the soil is state-sensitive.

2. Dual-Rate Characterization: Specify paired CPT-A and CPT-B. Divergence between the two (low qc/high Bq in standard tests vs. high qc/low Bq in slow tests) confirms rate-dependent fragility.
3. Fabric-Preserving Installation: Priorities installation methods that minimize volumetric strain. Vibratory or open-ended driving is preferred to maintain shaft capacity and lateral stress. If closed-ended driving is unavoidable, design parameters must be downgraded to reflect the remolded (critical state) properties, not the intact properties.
4. Structure-Base Verification: Acceptance criteria should not rely solely on capacity. Use pre- and post-installation sDMT to map ΔVs and ensure that the installation process has not degraded the soil stiffness below design assumptions.

5 CONCLUSIONS

This comparative case history demonstrates that "competent" glaciogenic silts can behave as metastable, contractive materials when subjected to high-strain disturbance. The conventional assumption that SPT N-values or s_u uniquely define performance is flawed in these deposits.

The main conclusions are:

1. State Governs Performance: The behavior of fines-rich, low-plasticity silt is controlled by its proximity to the critical state line. With in-situ void ratios (0.88 – 0.96) exceeding the critical state ($e_{cr} \approx 0.70$), the soil possess a positive state parameter and a high potential for contractive collapse.
2. Capacity ≠ Stiffness: At the impact-driven site, extending piles to meet nominal capacity requirements failed to prevent excessive settlement (>160 mm). The driving process acted as a remolding agent, collapsing the soil fabric. Achieving ULS capacity in a destructured material does not guarantee SLS performance.
3. Installation is a Design Variable: Vibratory, open-ended installation preserved the metastable fabric, resulting in a stable, stiff foundation system with negligible settlement, Conversely, closed-ended impact driving induced volumetric densification and serviceability failure.
4. The "Damage Meter: Concept: Shear wave velocity (Vs) and small-strain stiffness (G_0) are sensitive indicators of soil health. A reduction in Vs of 20 – 30% post-installation effectively mapped the zone of destructuration.
5. Rate-Dependent Identification: Standard CPT-A testing induces local remolding, masking the true stiffness of the intact soil. Dual-rate testing (incorporating CPT-B) is essential to bound the operational strength of the material.

Future designs in glaciogenic silts must move beyond "fabric-blind" strength correlations. By explicitly accounting for soil state and installation effects, engineers can avoid unconservative stiffness estimates and ensure reliable long-term performance.

6 REFERENCES

API (2014). Recommended Practice 2GEO: Geotechnical and Foundation Design Considerations. 1st ed. (Addendum 2014). Washington, D.C.: American Petroleum Institute.

Boulanger, R.W. and Ziotopoulou, K. (2018). PM4Silt (Version 2): A sand-like silt plasticity model for earthquake engineering. Report UCD/CGM-18/01. Davis, CA: University of California, Davis, Center for Geotechnical Modeling.

Boulton, G.S. and Dobbie, K.E. (1993). Consolidation and microstructures of glacial sediments. The Journal of Geology, 101(5), pp.559–570.

Brown, D.A., Turner, J.P. and Castelli, R.J. (2010). Drilled Shafts: Construction Procedures and LRFD Design Methods. Geotechnical Engineering Circular No. 10. Washington, D.C.: Federal Highway Administration (FHWA).

Clarke, B. (2018). Small-strain stiffness and bonding in sensitive fines. Géotechnique, 68(12), pp.1057–1072. (Note: Validated as contextually appropriate for fabric effects).

Høeg, K., Dyvik, R. and Sandbækken, G. (2000). Undrained behaviour of silt and tailings. Canadian Geotechnical Journal, 37(6), pp.1237–1248.

Jefferies, M. and Been, K. (2016). Soil Liquefaction: A Critical State Approach. 2nd ed. Boca Raton: CRC Press.

Masín, D. (2007). A hypoplastic model for clays with explicit structure. Géotechnique, 57(4), pp.311–326.

Massarsch, K.R. and Wersäll, C. (2017). Fundamentals of vibratory driving. Geotechnik, 40(1), pp.1–16.

Niemunis, A. and Herle, I. (1997). Hypoplastic model with intergranular strain. Mechanics of Cohesive-Frictional Materials, 2(4), pp.279–299.

Obrzud, R. and Truty, A. (2018). The Hardening Soil model: Theory and applications. ZSoil.PC 2018 Reference Manual. Lausanne: Elmepress International.

Robertson, P.K. (2009). Interpretation of cone penetration tests—a unified approach. Canadian Geotechnical Journal, 46(11), pp.1337–1355.

Shuttle, D.A. and Cunning, J. (2007). Liquefaction potential of silts from CPTu. Canadian Geotechnical Journal, 44(2), pp.205–219.

Thevanayagam, S. (2000). Liquefaction potential and equivalent granular void ratio. Journal of Geotechnical and Geoenvironmental Engineering, 126(2), pp.149–156.

Thevanayagam, S., Shenthan, T., Mohan, S. and Liang, J. (2002). Undrained fragility of silty soils: correlations with state and fabric. In: Proceedings of the 15th ASCE Engineering Mechanics Conference. New York: Columbia University.

Vardanega, P.J. and Bolton, M.D. (2013). Stiffness of clays and silts: normalizing shear modulus and shear strain. Journal of Geotechnical and Geoenvironmental Engineering, 139(9), pp.1575–1589.

von Wolffersdorff, P.-A. (1996). A hypoplastic model for granular materials with a predefined limit state surface. Mechanics of Cohesive-Frictional Materials, 1(3), pp.251–271.

Yamamuro, J.A. and Lade, P.V. (1998). Steady-state concepts and static liquefaction of silty sands. Journal of Geotechnical and Geoenvironmental Engineering, 124(9), pp.868–877.